

# MULTIFUNCTIONAL COMPOSITES: MODELING INTERCALATION INDUCED STRESSES IN CONSTITUENTS OF MICRO-BATTERY

Johanna Xu<sup>1</sup>, Andrejs Pupurs<sup>1</sup>, Göran Lindbergh<sup>2</sup> and Janis Varna<sup>1</sup>

<sup>1</sup>Department of Engineering Sciences and Mathematics, Luleå University of Technology SE-97187  
Luleå, Sweden

<sup>2</sup>KTH Royal Institute of Technology, School of Chemical Science and Engineering, SE - 100 44  
Stockholm, Sweden

**Keywords:** Micro battery, Carbon fibers, Lithium ion, Intercalation, Expansion, Stress state

## Abstract

A structural battery that simultaneously carries mechanical loads while storing electrical energy offers the potential of significantly reduced total vehicle weight owing to the multifunctionality. Carbon fiber is employed as negative electrode of the battery and also as a composite reinforcement material. It is coated with a solid polymer electrolyte working as an ion conductor and separator whilst transferring mechanical loads. The coated fiber is surrounded by a conductive positive electrode material. This paper demonstrates a methodology for addressing mechanical stresses arising in a conceptualized micro battery cell during electrochemical cycling, caused by time dependent gradients in lithium ion concentration distribution in the carbon fiber.

## 1. Introduction

A structural composite battery that undertakes the two roles of electrical energy storage and mechanical load bearing enables significant weight savings [1].

To design structural energy storage composite, carbon fiber is used for its load carrying properties and also for its electrical conduction and lithium-ion ( $\text{Li}^+$ ) intercalation ability. For mechanical performance the liquid electrolyte commonly used in conventional batteries needs to be replaced with a solid polymer electrolyte (SPE), acting as an ion conductive medium as well as transferring load in the composite material. A major drawback for using SPE in structural battery is the decreased ion conductivity with increased material stiffness. However, the effect of low ion conductivity can be overcome by utilizing so called micro battery cell design, where the thickness of the electrolyte is reduced to a less than  $1\mu\text{m}$  by electropolymerization [2].

Within this conceptualized micro battery cell design, in each repeating unit the negative electrode consists of one single carbon fiber, coated with a thin layer of SPE and an additional layer with the positive electrode.

During electrochemical cycling the constituents of the 3-cylinder unit undergo volume changes due to the migration of lithium ions between them. These volume changes together with the applied mechanical load affect the internal stress state, potentially causing micro damage formation in the material, which results in electrical and mechanical performance degradation.

The  $\text{Li}^+$  diffusion in a carbon fiber and the resulting internal stresses, possibly causing damage formation has been studied by Pupurs et al [3], with the simplification that the fiber is surrounded by an infinite source of  $\text{Li}^+$ .

The objective of this paper is to investigate the mechanical stress fields arising during two different types of battery operation, fast and slow discharge rate, respectively. The  $\text{Li}^+$  diffusion in the carbon fiber is assessed by modeling all physical events present in the battery system.

Johanna Xu, Andrejs Pupurs, Göran Lindbergh and Janis Varna

## 2. Theoretical background

### 2.1 Mechanisms in liquid electrolyte battery

In a typical Li-ion cell there are four main components, (Fig 1), the negative electrode connected to the negative terminal of the cell, the positive composite electrode connected to the positive terminal of the cell, and a separator and electrolyte between the two electrodes. In the negative electrode lithium is stored in the lattice sites made from graphite. The positive electrode usually consists of a mixture of lithiated metal oxide or metal phosphate, electronic conductor additives and polymer binder.

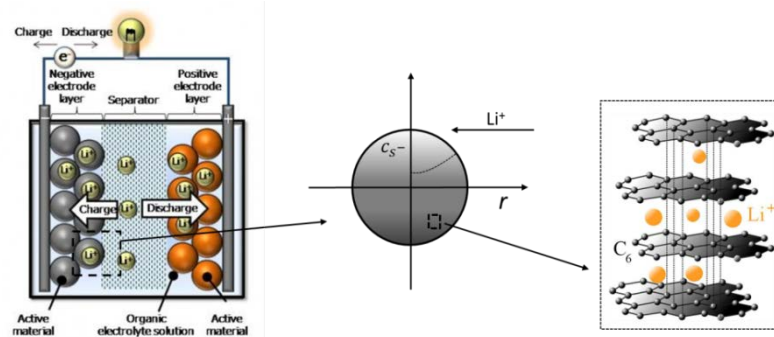


**Figure 1.** Schematics of Li-ion cell different length scales. [4]

When a lithium-ion battery is in use, i.e. during discharge,  $\text{Li}^+$  ions diffuse to the surface of  $\text{Li}_x\text{C}_6$  active material particles in the negative electrode where they undergo electrochemical reactions and transfer into a liquid electrolyte solution.

Then the positively charged  $\text{Li}^+$  ions travel through the electrolyte solution via diffusion and ionic conduction to the positive electrode where they react and diffuse towards the inner regions of the metal phosphate active material particles.

Likewise, during charging, the  $\text{Li}^+$  ions travel from the positive electrode lattice sites to the lattice sites in the negative electrode. This process is called intercalation, (Fig 1).

The separator serves as an electric insulator to avoid short circuiting, by forcing electrons through an external circuit of load, whilst allowing the  $\text{Li}^+$  ions to pass through it during battery operation.

Lithium is considered to exist in two separate states, called phases: (i) the active material (solid phase) in the electrode material and (ii) the liquid phase in the dissolved state in the electrolyte.

### 2.2 Solid electrolyte battery cell design and geometry

The conceptualized cylindrical battery cell consists of an individual negative electrode, carbon fiber coated by a gel electrolyte (lithium salt and solvent dissolved in a polymer) material surrounded by a solid positive electrode material, which partially consist of the electrochemically active material  $\text{LiFePO}_4$ , i.e. the  $\text{Li}^+$  host material, denoted with index  $a$  in section 2.4.

The total radius of the battery system is  $4.3\mu\text{m}$ , detailed dimensions are shown in Table 1 and (Fig 2).

**Table 1.** Battery cell constituents

Constituent	Thickness
Carbon fiber, $r_f$	$2.5\mu\text{m}$
Polymer/gel layer on carbon fiber, $r_c - r_f$	$0.1\mu\text{m}$
Positive electrode matrix, $r_m - r_c$	$1.7\mu\text{m}$

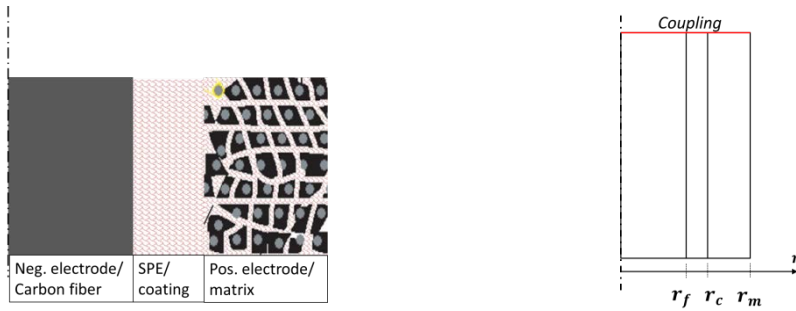


**Figure 2.** a) Schematics of micro battery constituents. b) Model geometry.

### 2.3 Stresses in micro-battery cell

Lithium intercalation leads to changes in the crystal lattice of the carbon fiber microstructure, both in the direction of basal planes and interplane, resulting in dimensional changes of the carbon fiber, experimentally observed in [5].

The intercalation induced stresses in a transversely isotropic active material can be considered through a thermo-mechanical analogy [3].

In the linear elasticity theory these dimensional changes are assumed to be proportional to the  $\text{Li}^+$  concentration,  $c$ . For a transverse isotropic material, two different constant coefficients of proportionality called intercalation-expansion coefficients are required to characterize the dimensional changes in the three directions.

$$\sigma_i^k = C_{ij}^k \left( \varepsilon_j^k - \beta_j \frac{c_k}{c_{k,max}} \right) \quad k = f, c, m \quad (1)$$

where index  $k = m$  for the matrix,  $k = c$  for the coating, and  $k = f$  for the fiber, and  $i, j = r, \theta, z$  are cylindrical coordinates.

Here  $\beta_j \frac{c_k}{c_{k,max}}$  is the free swelling strain in  $j$ -direction due to Li-ion intercalation, which is included in the elastic stress-strain relationship. In the concentric micro battery cell, where the concentration distribution is not uniform and the carbon fiber is constrained by the battery constituent materials, intercalation induces stresses.

For a transversally isotropic material  $C_{13} = C_{12}, C_{22} = C_{33}, \beta_r = \beta_\theta$ .

For an axi-symmetric problem, (Fig 2b), assuming an infinite long fiber, when all shear stress components are equal to zero, the only non-trivial equilibrium equation is

$$\frac{\partial \sigma_r^k}{\partial r} + \frac{\sigma_r^k - \sigma_\theta^k}{r} = 0 \quad (2)$$

The strain relationship to radial displacement  $u_r$  is given by

$$\varepsilon_r^k = \frac{\partial u_r^k}{\partial r} \quad \varepsilon_\theta^k = \frac{u_r^k}{r} \quad \varepsilon_1 = \varepsilon_{10} = \varepsilon_{1f} = \varepsilon_{1m} = \varepsilon_{1c} \quad (3)$$

The displacement and stress solutions obtained for each phase separately must satisfy the following interface conditions:

- (i) Radial displacement must be zero on the symmetry axis.
- (ii) Radial displacement and stress continuity conditions at all interfaces.
- (iii) Outer boundary of the cylinder assembly is stress free.

## 2.4 Lithium ion concentration distribution in carbon fiber

The lithium ion transportation in the negative electrode, which is composed exclusively of the active material, the carbon fiber, is described by Fick's law of diffusion

$$\frac{\partial c_f}{\partial t} = \nabla \cdot (D_f \nabla c_f) \quad (4)$$

where subscript  $f$  denotes the fiber phase,  $D$  is the diffusion coefficient,  $t$  is the time, and  $\nabla$  is the Nabla operator.

With boundary conditions

$$-D_f \frac{\partial c_f}{\partial r} \Big|_{r=0} = 0 \quad -D_f \frac{\partial c_f}{\partial r} \Big|_{r=r_f} = J_f(t) \Big|_{r=r_f} \quad (5)$$

where  $r_f$  is the carbon fiber radius,  $J_f$  is the molar flux at the carbon fiber surface describing the process kinetics by linking the current density, ion concentration and overpotential. The electrochemical reaction kinetics yielding the molar flux  $J_f$  at the electrode surface is given by the Butler-Volmer equation

$$J_f \Big|_{r=r_f} = i_{0,f} \left[ \exp\left(\frac{\alpha_a F \eta_f}{R_g T}\right) - \exp\left(-\frac{\alpha_c F \eta_f}{R_g T}\right) \right] \quad (6)$$

where  $i_{0,f}$  is a material property termed exchange current density which is the rate of oxidation and reduction at equilibrium,  $\alpha_a = 0.5$  and  $\alpha_c = 0.5$  are the electrochemical reaction symmetry factors, and  $\eta_f$  is the overpotential defined as:

$$\eta_f \Big|_{r=r_f} = \Phi_{s,f} - \Phi_{e,c} - E_{OCP,f} \quad (7)$$

where  $\Phi_{e,c}$  is the electrolyte phase electric potential in the SPE coating and  $\Phi_{s,f}$  is the solid phase electrical potential for the fiber, at the electrode/electrolyte interface, the  $E_{OCP}$  is the electrode equilibrium potential, a material property describing the potential observed experimentally at zero current.

Similar equations are describing the ion concentration in the active material of the matrix and the flux on the surface of the active material in the matrix.

The solid phase electric potential,  $\Phi_{s,k}$ , ( $k = f, m$ ), is calculated by Ohm's law describing the relation between the electric field, current density and material resistivity in the battery cell, with the applied current density as boundary condition

$$-\sigma_{eff,m} \frac{\partial \Phi_{s,m}}{\partial r} \Big|_{r=r_m} = I \quad (8)$$

where the current density  $I$  is related to the applied current  $i_{app}$  and the surface area of the battery,  $A$  as

$$I = i_{app}/A \quad (9)$$

The current is applied in terms of C-rates, with 1C defined as the required current to obtain full charge or discharge in 1 hour.

It has to be realized that in order to assess lithium ion concentration distribution in the carbon fiber (negative electrode),  $c_f$ , eq. (4), also electrolyte phase charge and mass balances need to be described. The macroscopic modeling of the mass transport in the electrolyte is adapted from work by Nyman et al [6].

In summary, the model to describe the ion concentration distribution in this micro battery unit cell consists of a coupled system of 11 nonlinear partial differential equations (PDE) with 11 unknowns,

which are: 2 active material concentrations  $c_f, c_a$ , 2 concentrations in the polymer electrolyte coating containing both salt and solvent  $c_{salt,c}, c_{solvent,c}$ , 2 concentrations in the matrix material consisting partially of the polymer electrolyte,  $c_{salt,m}, c_{solvent,m}$ , 3 potentials  $\Phi_{e,c}, \Phi_{e,m}, \Phi_{s,m}$ , and 2 fluxes  $J_f$  and  $J_m$ .

## 2.5 Input parameters

The electrochemical properties for the carbon fiber (negative electrode) are extracted from [7]. The electrochemical properties of the SPE are adopted from an extensive characterization study for a gel polymer in [6]. Both the composition and the electrochemical properties for the positive electrode material are assumed to correspond to [8].

The experimentally measured diffusion coefficient of the carbon fiber [7] shows strong concentration dependence,  $D = D(c)$ , ranging over three orders of magnitudes. The diffusion coefficient and the charge rate are studied by adopting two different values (low and high), Table 2.

**Table 2.** Parameters used in this study.

Parameter	low	high
Diffusion coeff. of carbon fiber	$D = 10^{-14} m^2/s$	$D = 10^{-11} m^2/s$
Charge rate (per 1m carbon fiber)	$0.1C = (1.63 \mu A)$	$10C = (0.163 mA)$

The input parameters used for the mechanical model are listed in Table 3. The free swelling strain in fiber axial direction was obtained by fitting experimental data from [5]. The macroscopic transverse swelling coefficient for carbon fibers is not available in literature, but have been approximated from measurements [5].

**Table 3.** Elastic constants and expansion coefficients of constituents.

Constituent	$E_z$ (GPa)	$E_r$ (GPa)	$\nu_{zr}$ (-)	$\nu_{r\theta}$ (-)	$G_{zr}$ (GPa)	Expansion	
						$\beta_z(-)$	$\beta_r(-)$
Fiber	300	30	0.2	0.45	20	0.009	0.05
SPE coating	1	1	0.3	0.3	0.38	0	0
matrix	3	3	0.3	0.3	1.15	0	0

The expansion coefficients  $\beta_z^c = \beta_z^m = \beta_r^c = \beta_r^m = 0$  means that no macroscopic swelling due to intercalation is anticipated. Actually, swelling in the active material particles of the matrix does occur, causing a change in volume fraction of the active material in the matrix, but the overall expansion of the matrix is zero. Swelling of the coating is neglected, because the properties are unknown, and the stiffness is very low, hence insignificant influence expected.

## 2.6 COMSOL Model

COMSOL Multiphysics 5.1 is employed to model the corresponding concentration distributions during  $Li^+$  intercalation and deintercalation. The electrochemical model is formulated for a cylindrical coordinate system, to describe the  $Li^+$  diffusion in and out of the electrodes in conjunction with appropriate boundary conditions, which are for space limitation not presented here.

A 2D axisymmetric representation is used to model the three concentric phases, the mechanical stresses are obtained by assuming generalized plane strain conditions,  $\varepsilon_z = const$ . Further, the carbon fiber is considered stress free with no lithium ions present. i.e. at fully discharged state.

### 3. Results and discussion

In (Fig 3a) it can be seen that the overpotential  $\eta$ , i.e. the electrochemical driving force for the reaction, defined in (eq. 7), at the carbon fiber surface is unaffected by the variation in diffusion coefficient for a slow discharge rate. However, for a fast discharging of 10C, (Fig 3b), the overpotential starts to increase rapidly in a much earlier stage of the discharge cycle for the case of slow diffusion coefficient in comparison with a fast diffusion, leading to large flux  $J_f$ , (eq. 6) at the fiber surface. If the time for transport is larger than the time for reaction, then the concentration gradient starts to build up between the electrode surface and the bulk of the electrolyte, resulting in increased resistance, hence a decrease in capacity (the amount of electric charge received or delivered by the cell) can be expected.

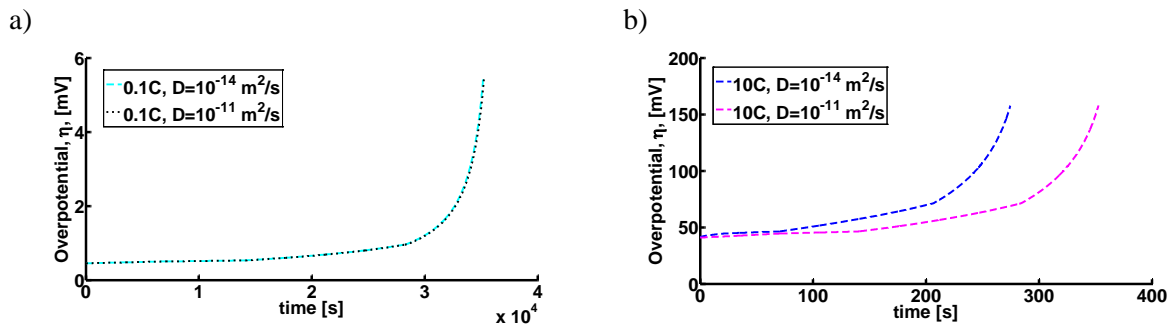


**Figure 3.** The overpotential, a) for a discharge rate of 0.1C. b) for a discharge rate of 10C.

The relationship between the lithium ion concentration in the carbon fiber center and at the carbon fiber surface, for the case corresponding to a fast discharge rate with slow diffusion, from a fully charged state to a completely discharged state is shown (Fig 4), the difference in  $\text{Li}^+$  concentration is prominent.

For the cases corresponding to a slow discharge rate with fast diffusion, slow discharge rate with slow diffusion, and fast discharge rate with fast diffusion the difference in ion concentration between fiber surface and center is minimal. The reason being that at a slow discharge rate, the flux is low, thus time is not a limiting factor, resulting in an insignificant effect of diffusion coefficient. At high discharge rate the difference  $\text{Li}^+$  concentration at fiber surface and center is very small, however, only in the case of fast diffusion coefficient which allows fast transportation without the appearance of gradients.

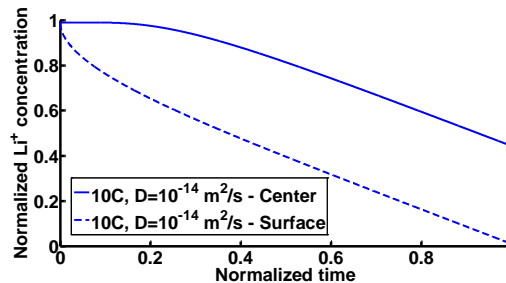


**Figure 4.** Lithium ion concentration in the carbon fiber electrode center and surface, respectively, for the cases of slow and fast discharging, with slow and fast diffusion coefficients respectively for the complete discharging time.

This difference in ion concentration between the fiber center and fiber surface is the cause for gradients in the stress distributions in the fiber. The two most extreme cases are examined, case (i) slow discharge rate with fast diffusion and case (ii) fast discharge rate with slow diffusion.

In (Fig 5) the ion concentration distributions along the radial direction corresponding to discharging/deintercalation are shown. (Fig 5a) show the distribution profiles for case (i), where the

concentration distribution is uniform for all time instances, until the final value of the concentration is zero at time for fully discharged state,  $t_d$ . For case (ii), (Fig 5b), gradients are noticeable, and the ions are still present in the fiber at 100% discharged state.

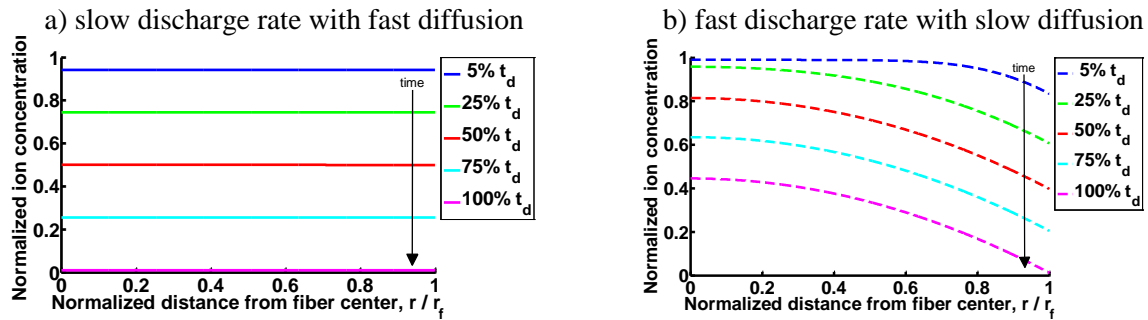


**Figure 5.** Distribution of ion concentration at for 5% (blue), 25% (green), 50% (red), 75% (cyan) and 100% (magenta) of the complete discharge time for a) slow discharge rate with fast diffusion (solid lines). b) fast discharge rate with slow diffusion coefficient (dashed lines)

### 3.1 Stresses in carbon fiber

The radial stress  $\sigma_r$ , hoop stress  $\sigma_\theta$  and axial stress  $\sigma_z$  in the fiber are presented in (Fig 6) for the cases corresponding to (i) slow discharge rate with fast diffusion (solid lines) and (ii) fast discharge rate with slow diffusion (dashed lines) during discharging.

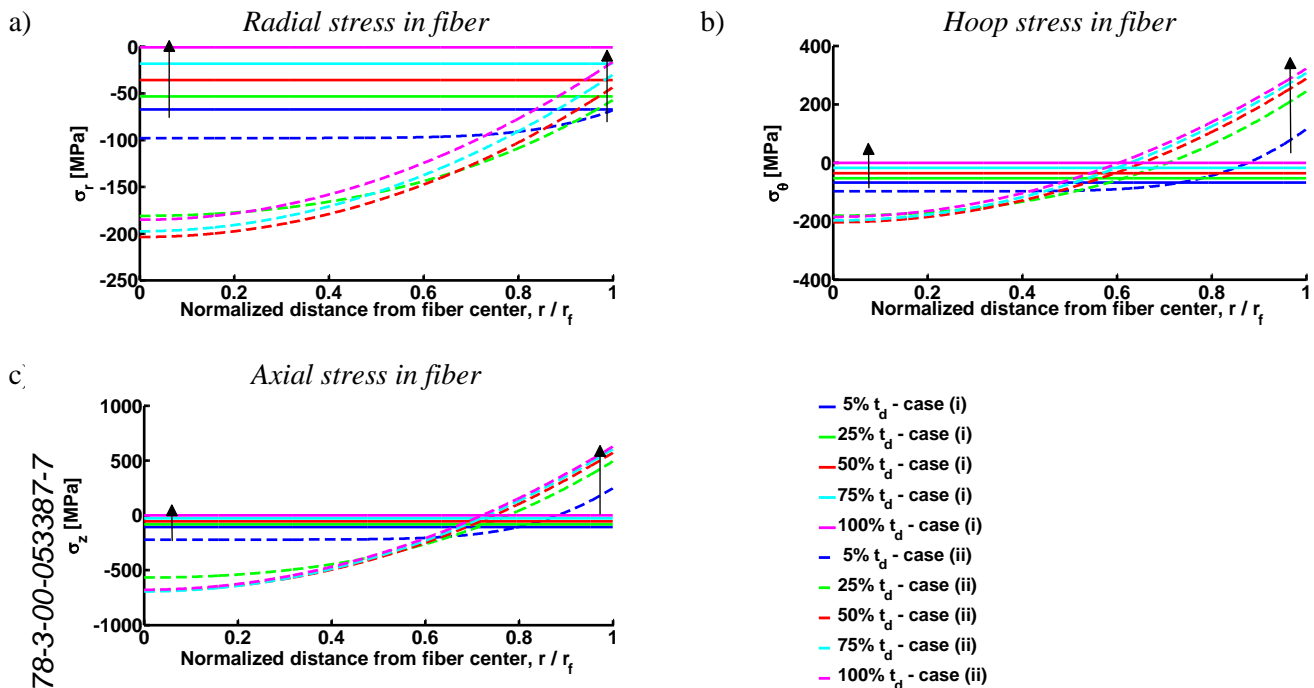


**Figure 6.** Stress distribution during discharge for 5% (blue), 25% (green), 50% (red), 75% (cyan) and 100% (magenta) of the complete discharge time. solid lines show slow discharge rate with fast diffusion coefficient, dashed lines show fast discharge rate with slow diffusion.

In case (i) the radial stress  $\sigma_r$ , the hoop stress  $\sigma_\theta$  and the axial stress  $\sigma_z$  is negative with uniform distribution, as a result of no concentration gradients, and values of these stresses are relatively low

and approach to zero with discharging. However for case (ii), dashed lines in (Fig 6), it can be seen that higher gradients in concentration results in higher values of the stress components. The radial stress is negative for all time instances in the fiber. The hoop stress and axial stress are negative in the inner region of the fiber but become positive towards the fiber/SPE interface. As the outer region, close to the fiber/SPE interface, which contains less Li<sup>+</sup> ions attempts to contract in the  $\theta$  direction, it is constrained by the inner region which due to the high concentration of ions, contracts much less, resulting in tensile stresses in the outer region and compressive stresses in the inner region.

#### 4. Conclusion

Lithium ion diffusion in a carbon fiber was analyzed numerically by a physics based electrochemical model; the resulting transient ion concentration distributions were used in combination with FEM based elastic stress analysis in order to assess the mechanical stresses in the fiber caused by non-uniform swelling. The result shows that a high charge rate has different effect on the stress state in the carbon fiber dependent on its diffusion coefficient.

Future studies involve using this model to address stresses under combined mechanical and electrochemical loading, and to evaluate possible damage mechanisms under different loading conditions.

#### Acknowledgments

The Swedish Energy Agency, project 37712-1 is acknowledged for financial support. KOMBATT-II project members are acknowledged for fruitful discussions.

#### References

- [1] Asp LE, Greenhalgh ES. Structural power composites. *Composites Sci Technol* 2014;101:41-61.
- [2] Leijonmarck S, Carlson T, Lindbergh G, Asp LE, Maples H, Bismarck A. Solid polymer electrolyte-coated carbon fibres for structural and novel micro batteries. *Composites Sci Technol* 2013;89:149-157.
- [3] Pupurs A, Varna J. Modeling mechanical stress and exfoliation damage in carbon fiber electrodes subjected to cyclic intercalation/deintercalation of lithium ions. *Composites Part B* 2013.
- [4] Hitachi Ltd. 2015;2016(04/01).
- [5] Jacques E, Hellqvist Kjell M, Zenkert D, Lindbergh G, Behm M. Expansion of carbon fibres induced by lithium intercalation for structural electrode applications. *Carbon* 2013;59:246-254.
- [6] Nyman A, Behm M, Lindbergh G. A theoretical and experimental study of the mass transport in gel electrolytes II. Experimental characterization of LiPF<sub>6</sub>-EC-PC-P(VdF-HFP). *J Electrochem Soc* 2011;158(6):A636-A643.
- [7] Kjell MH, Zavalis TG, Behm M, Lindbergh G. Electrochemical characterization of lithium intercalation processes of PAN-based carbon fibers in a microelectrode system. *J Electrochem Soc* 2013;160(9):A1473-A1481.
- [8] Zavalis TG, Klett M, Kjell MH, Behm M, Lindström RW, Lindbergh G. Aging in lithium-ion batteries: Model and experimental investigation of harvested LiFePO<sub>4</sub> and mesocarbon microbead graphite electrodes. *Electrochim Acta* 2013;110:335-348.